Rock Mechanics 5, 215—230 (1973)

Indirect Tensile Testing of Anisotropic Rocks

By

G. Barla and **N. Innaurato**

With 16 Figures

(Received November 27, 1972)

Summary — Zusammenfassung — Résumé

Indirect Tensile Testing of Anisotropic Rocks. The tensile strength of rock materials is a parameter relevant to many rock mechanics applications. Rocks are often anisotropic in nature. Therefore, it is of interest to investigate suitable experimental methods for tensile testing to be used with these rocks. An attempt is made in this paper to see if the indirect methods adopted for testing isotropic rocks can be applied. Two rock types with transversely isotropic behavior are tested by loading discs and rings along their diameter. The finite element method is used in order to correlate the tensile stress, for which tensile failure is assumed to occur in each test, with the orientation of the axes of anisotropy. It is shown that the experimental results can be appropriately explained by this method and a parameter be defined which allows one to describe the law of variation of tensile strength with the anisotropy of deformability.

Indirekte Zugfestigkeitsprüfung anisotroper Gesteine. Die Zugfestigkeit eines Gesteins stellt bei felsmechanischen Betrachtungen einen wichtigen Parameter dar. Die bisherigen Wege, diesen Parameter zu erfassen, setzen ein isotropes, homogenes Medium voraus. Da der natürliche Fels stets anisotrop und inhomogen ist, prüfen die Autoren die Möglichkeit, indirekte Zugversuche, wie sie bisher angewandt wurden, auf anisotrope Medien zu übertragen.

Die Autoren untersuchen das Verhalten von Granitgneis und Serpentinschiefer mit Transversal-Anisotropie. Die Untersuchung erfolgt im Druckversuch an Scheiben und Ringen längs des vertikalen Durchmessers, wie es für homogenes und isotropes Material im Sinne der klassischen Elastizitätstheorie üblich ist.

Durch Anwendung der Finite-Element-Methode gelingt es, die Beziehungen zwischen Bruch-Zugspannung und Abweichung der Anisotropie-Achse zu ermitteln.

Auf diesem Wege werden die experimentellen Ergebnisse erklärbar. Darüber hinaus ist es möglich, einen Parameter zu bestimmen, der es erlaubt, einen gesetzmäßigen Zusammenhang zwischen der Zugfestigkeit und dem Grad der Anisotropie des Gesteins zu ermitteln.

Essais indirects de traction sur des roches anisotropes. La connaissance de la contrainte de traction à la rupture est un paramètre important dans le domaine de la Mécanique des Roches. Etant donné que la plupart des roches sont anisotropes, il est intéressant de développer des essais capables de donner la contrainte de

rupture à la traction de ces roches. Dans ce travail on a cherché à vérifier si les essais indirects de traction utilisés depuis longtemps pour des roches isotropes sont valables aussi pour des roches anisotropes. Dans ce but on a examiné le comportement de deux types de roche à isotropie transversale en exécutant des essais de compression le long d'un diamètre sur des disques et des anneaux. La méthode des éléments finis a été appliquée dans le but de disposer d'une corrélation entre la contrainte de traction pour laquelle la rupture a lieu, avec l'orientation de l'axe d'anisotropie. On a ainsi déduit que les résultats expérimentaux peuvent être interprétés par cette méthode et qu'il est possible aussi de définir un paramètre qui permet d'en tirer une loi de variation de la résistance à la traction en fonction de l'anisotropie de la déformabilité.

Introduction

The diametral compression of circular discs and rings is a well known method for determining the tensile strength of rock materials. This method is generally applied to homogeneous and isotropic rocks, as the formulae which are used for calculation are based upon the assumptions of the Classical Theory of Elasticity.

Anisotropic rocks are seen to occur in many practical applications. However, experimental evidence on the behavior of rocks of this type, when subjected to tensile stress, is limited (Hobbs, 1964). Furthermore, only a few theoretical investigations have been reported on this subject (Fine e Vouille, 1970; Barron, 1971).

It is the purpose of the present paper to analyse the problems which are to cope with in the interpretation of the experimental results obtained in testing two different rocks with anisotropic behavior. The finite element method is used in order to correlate the tensile stress, for which tensile failure is assumed to occur, with the orientation of the principal axes of anisotropy.

Experimental Results

Two rock types have been selected for these experiments: a granitoidic gneiss from Valle di Susa (Susa, Italy) and a serpentinous schist from Val Malenco (Sondrio, Italy). These two rocks were chosen because they exhibit anisotropy both of deformability and strength. The representative mechanical properties, obtained for these rocks in uniaxial compression tests, are summarized in Table 1, where the indices 1 and 2 refer to the directions respectively parallel and perpendicular to the laminations.

a) Diametral compression of circular discs

A total of 52 circular discs (24 of granitoidic gneiss and 28 of serpentinous schist), 56 mm diameter (D) and 11 mm thickness (t), were tested in a suitable system which insured the diametral load P be applied carefully and uniformly. The specimens were loaded at different orientations, with respect to the laminations, defined in the following with the angle β of Fig. 1.

The results obtained in these tests are illustrated in Fig. 2 and 3 for the gneiss and in Fig. 4 and 5 for the schist. The ratio P_f/Dt (P_f is the value of P applied at failure) is shown to depend in both cases upon the value of β.

Table 1. Mechanical Properties in Uniaxial Compression Tests

Constants	Gneiss	Schist
E_1	430,000	580,000
E_2	370,000	270,000
ν_1	0.21	0.34
ν_2	0.21	0.12
$C_{o\,1}$	1,800	600
$C_{o\,2}$	1,200	930
E_1/E_2	1.12	2.14
ν_1/ν_2	1.00	3.00
$C_{o\,1}/C_{o\,2}$	1.50	0.63

$E_{1,2}$ = Young's modulus (kg/cm²);
$\nu_{1,2}$ = Poisson ratio;
$C_{o\,1,2}$ = Compressive strength (kg/cm²).

In all figures the solid curve represents a polynomial fitting the experimental results with higher degree of approximation. It is of interest to notice that the maximum value of P_f/Dt occurs in both cases for $\beta = 0^0$. The minimum value is found at $\beta = 60^0$ for the schist and at $\beta = 75^0$ for the gneiss.

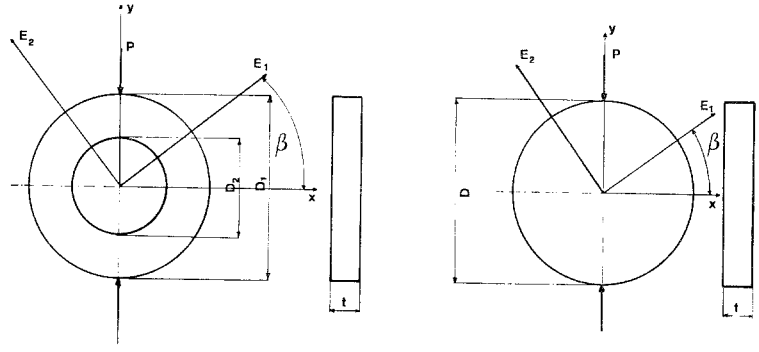

Fig. 1. Diametral compression of circular disc (right) and ring (left)
Schemazeichnung der Diametralversuche. Rechts: Scheiben; links: Ringe
Schéma des essais de compression le long d'un diamètre sur des disques (droite) et des anneaux (gauche)

The two rocks exhibit under testing two different trends of behavior. The gneiss fails mostly along the diameter of load application (Fig. 6). On the contrary, the schist is seen often to fail along the laminations (Fig. 7). This observation raises serious doubts on the nature of the failure process.

The failures, according to their occurrence on testing the 28 discs of schist, are reported in Table 2. An attempt is also made in Fig. 4 and 5 to

classify the type of failure by distinguishing it, when there is sufficient evidence, in tensile and shear.

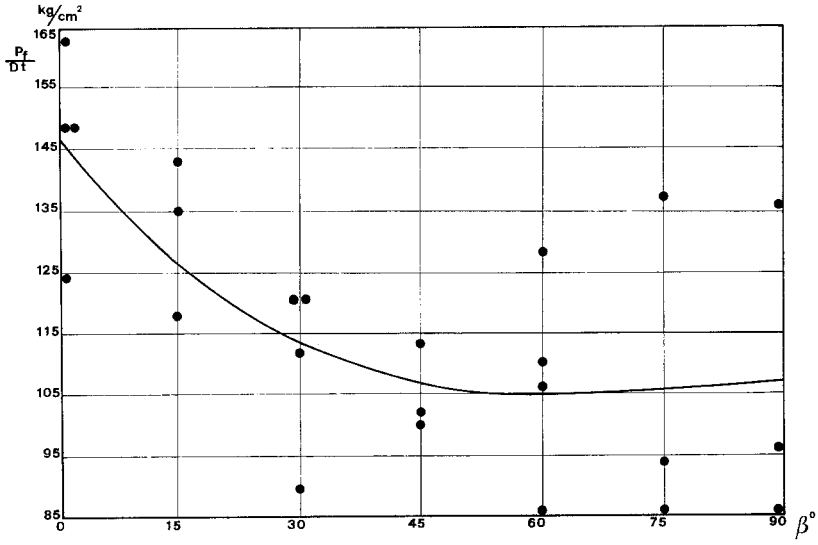

Fig. 2. Discs of granitoidic gneiss: experimental results. Ordinate, P_f/Dt; abscissa, β
Scheiben von Granitgneis: Versuchsergebnisse. Beziehung zwischen P_f/Dt und β
Disques de gneiss granitoïde: résultats des essais. Ordonnées, P_f/Dt; abscisses, β

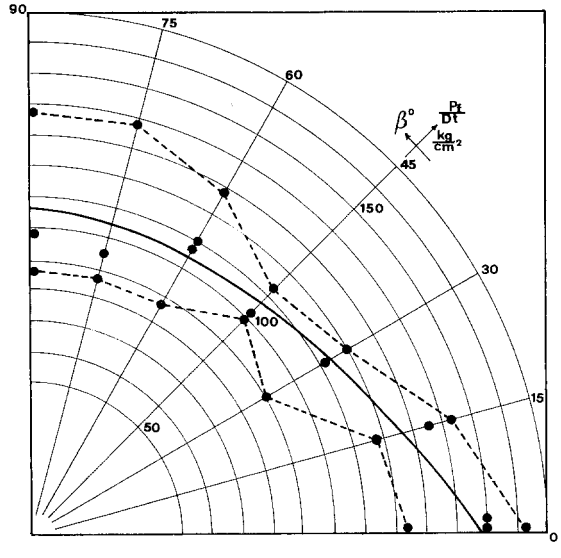

Fig. 3. Discs of granitoidic gneiss: experimental results. Polar diagram, P_f/Dt vs. β
Scheiben von Granitgneis: Versuchsergebnisse. Polar-Diagramm zwischen P_f/Dt und β
Disques de gneiss granitoïde: résultats des essais. Courbe polaire, P_f/Dt — β

This first series of experiments let one think that the tensile testing of anisotropic rocks by diametral loading of circular discs might be a suitable

Table 2. Type of Failure for Circular Discs of Serpentinous Schist

β (°)	Number of specimens which fail		
	Along line of loading	Along laminations	Otherwise
0	—	—	5
15	—	1	1
30	—	3	2
45	—	4	—
60	—	4	—
75	—	—	4
90	4	—	—

technique only for rocks which exhibit a moderate anisotropy (e. g. the granitoidic gneiss).

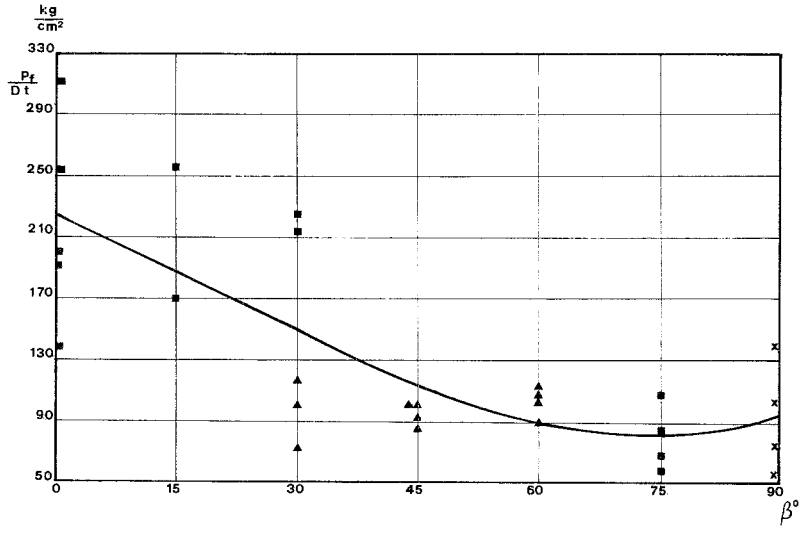

Fig. 4. Discs of serpentinous schist; experimental results. Ordinate, P_f/Dt; abscissa, β
× tensile failure, ▲ shear failure, ■ unknown failure

Scheiben von Serpentinschiefer: Versuchsergebnisse. Beziehung zwischen P_f/Dt und β
× Zugspannungbruch, ▲ Scherspannungbruch, ■ Bruch aus unbekannter Ursache

Disques de serpentine: résultats des essais. Ordonnées, P_f/Dt, abscisses, β
× rupture par traction, ▲ rupture par cisaillement, ■ rupture par une cause inconnue

However, even in this case a theoretical relationship must still be established in order to define the dependence of the tensile strength upon β. In fact, the known formula for tensile strength calculation ($T_0 = 2\,P_f/\pi D t$), based upon the Classical Theory of Elasticity, would not be applicable.

b) Diametral compression of circular rings

The result obtained for the schist asked for a different method of testing to be used in order to induce a true tensile failure in this rock.

Therefore, the diametral compression of circular rings was employed. 51 circular rings with 56 mm outside diameter (D_1), 34 mm inside diameter

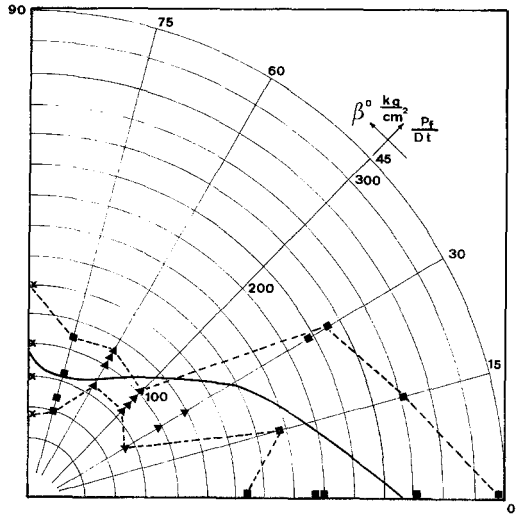

Fig. 5. Discs of serpentinous schist: experimental results. Polar diagram, P_f/Dt vs. β
× tensile failure, ▲ shear failure, ■ unknown failure

Scheiben von Serpentinschiefer: Versuchsergebnisse. Polar-Diagramm zwischen P_f/Dt und β
× Zugspannungbruch, ▲ Scherspannungbruch, ■ Bruch aus unbekannter Ursache

Disques de serpentine: résultats des essais. Courbe polaire $P_f/Dt - \beta$
× rupture par traction, ▲ rupture par cisaillement, ■ rupture par une cause inconnue

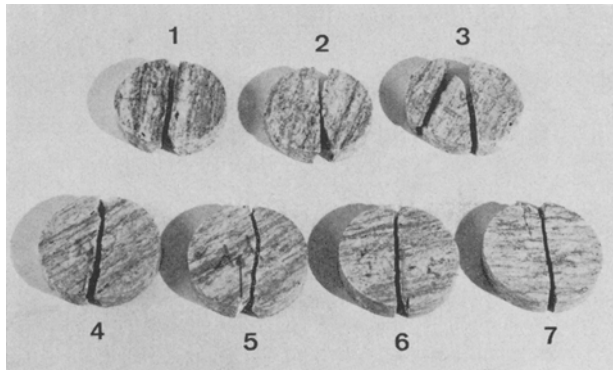

Fig. 6. Discs of granitoidic gneiss showing the type of failure
Brucharten der Scheiben von Granitgneis
Lignes de rupture des disques de gneiss

(D_2), and 11 mm thickness (t), were used. With the main purpose of ascertaining the influence of thickness, circular rings with the same cross section dimensions but 24 mm thickness were also tested.

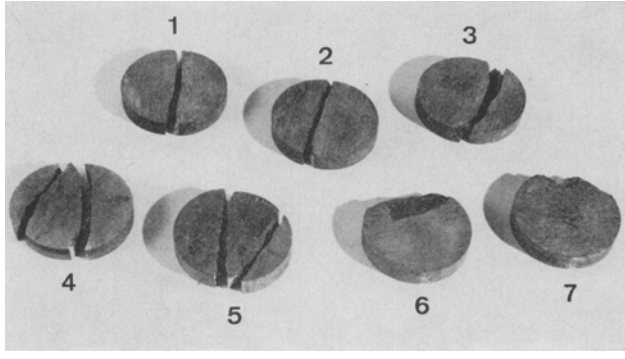

Fig. 7. Discs of serpentinous schist showing the type of failure
Brucharten der Scheiben von Serpentinschiefer
Lignes de rupture des disques de serpentine

The results are illustrated in the Figs. 8 to 10, where the values of $P_f/D_1 t$ are reported versus the angle β. The solid curve, shown in these figures, stands for the polynomial fitting the experimental results with higher degree of approximation. It is noticed that the dashed curve reported in Fig. 8 shows the same polynomial for the rings with a 24 mm thickness.

The ring thickness influences the results only slightly, as a maximum 10 per cent deviation in the value for $P_f/D_1 t$ is found among the two series of tests which were examined. A minimum for the curve $P_f/D_1 t$ vs. β occurs at $\beta = 75^0$, when $t = 11$ mm. The rings with a 24 mm thickness show, however, a minimum at $\beta = 90^0$.

Table 3. Summary of Observations Made in Testing Rings

β (°)	Number of specimens tested	Number of specimens which fail		
		Along line of loading	Along laminations	Otherwise
0	6	6	6	4
15	7	7	7	3
30	8	8	8	2
45	8	5	7	5
60	8	8	8	2
75	7	7	7	3
90	7	7	7	4

It can be noticed from the summary of the observations reported in Table 3 that the rings with smaller thickness generally fail first along the line of loading. Subsequently, new fractures arise along the laminations and, in

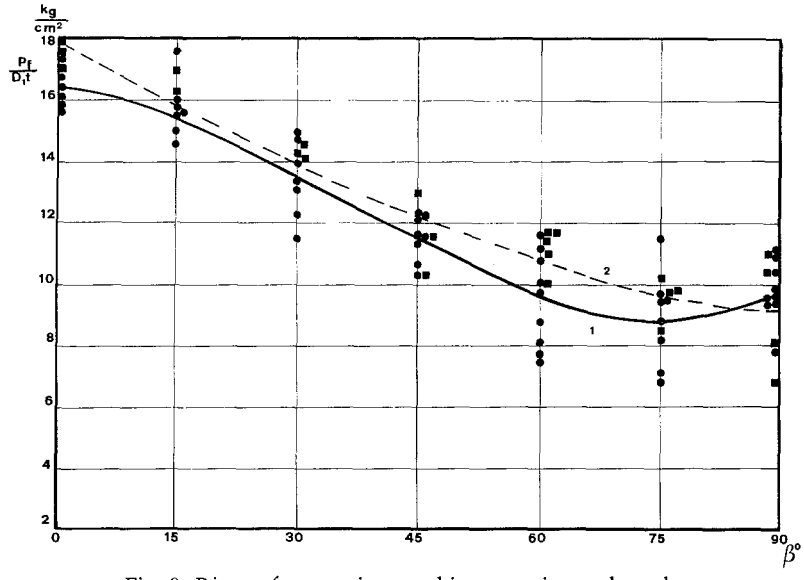

Fig. 8. Rings of serpentinous schist: experimental results
1. $t=11$ mm; 2. $t=24$ mm. Ordinate, $P_f/D_1\,t$; abscissa, β

Ringe von Serpentinschiefer: Versuchsergebnisse. Beziehung zwischen $P_f/D_1\,t$ und β
1. (Kreise): $t=11$ mm; 2. (Quadrate): $t=24$ mm

Anneaux de serpentine: résultats des essais
1. $t=11$ mm; 2. $t=24$ mm. Ordonnées: $P_f/D_1\,t$; abscisses: β

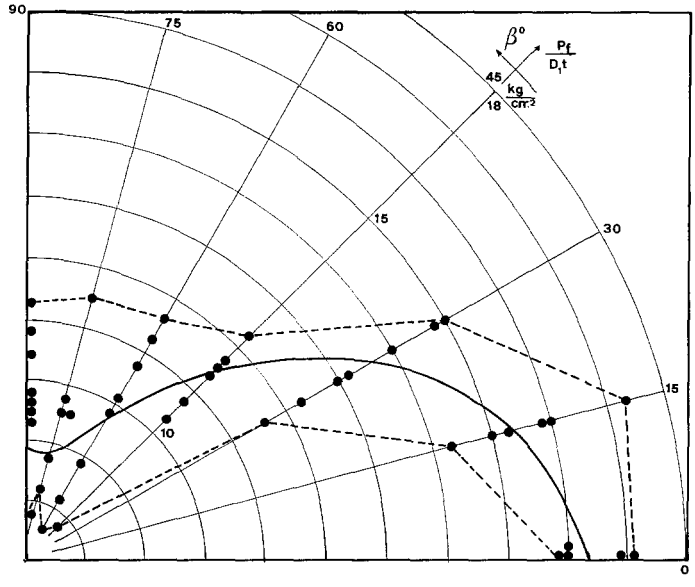

Fig. 9. Rings of serpentinous schist ($t=11$ mm): experimental results
Polar diagram, $P_f/D_1\,t$ vs. β

Ringe von Serpentinschiefer: ($t=11$ mm): Versuchsergebnisse
Polar-Diagramm zwischen $P_f/D_1\,t$ und β

Anneaux de serpentine ($t=11$ mm): résultats des essais. Courbe polaire $P_f/D_1\,t$ — β

some cases, fractures are also seen to develop at 5—15 degrees with respect to the laminations (Fig. 11).

Therefore, it can be concluded that the rocks which are markedly anisotropic (e. g. the serpentinous schist) can be tested for tensile strength

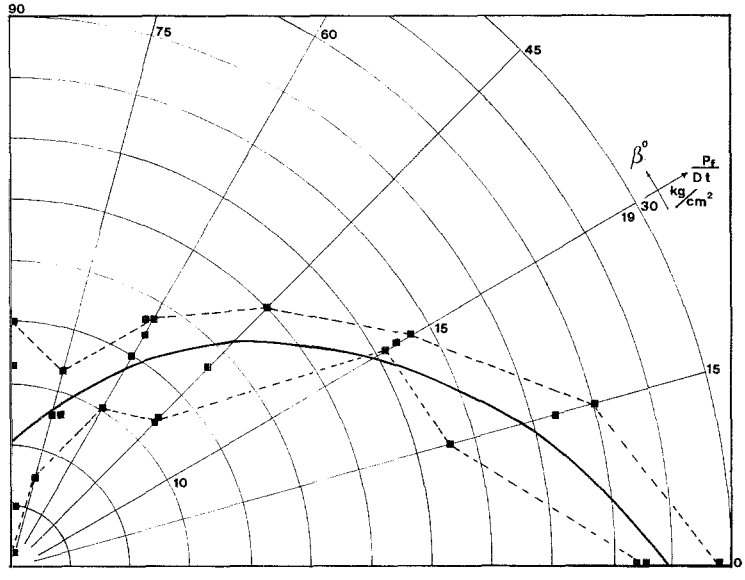

Fig. 10. Rings of serpentinous schist ($t=24$ mm): experimental results
Polar diagram, $P_f/D_1\, t$ vs. β

Ringe von Serpentinschiefer ($t=24$ mm): Versuchsergebnisse
Polar-Diagramm zwischen $P_f/D_1\, t$ und β

Anneaux de serpentine ($t=24$ mm): résultats des essais. Courbe polaire $P_f/D_1\, t$ — β

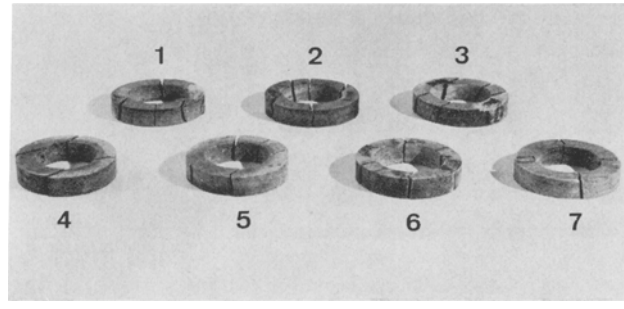

Fig. 11. Rings of serpentinous schist showing the type of failure

Brucharten der Ringe von Serpentinschiefer

Lignes de rupture des anneaux de serpentine

determination by using the diametral compression of circular rings. The necessity now arises again to find a theoretical relationship between the

tensile strength and β. The classical formula for tensile strength calculation ($T_0 = K_r\, 2\, P_f/D_1\, t$, K_r = stress coefficient given as function of D_1/D_2) is no longer applicable.

Theoretical Results

A theoretical study has been carried on, by using the finite element method, with the main purpose of finding out how the maximum tensile stress which develops in discs and rings can be correlated with the rock anisotropic behavior.

Two models, constructed by using triangular plane elements with three nodes, were employed. They are illustrated in Fig. 12. The boundary and

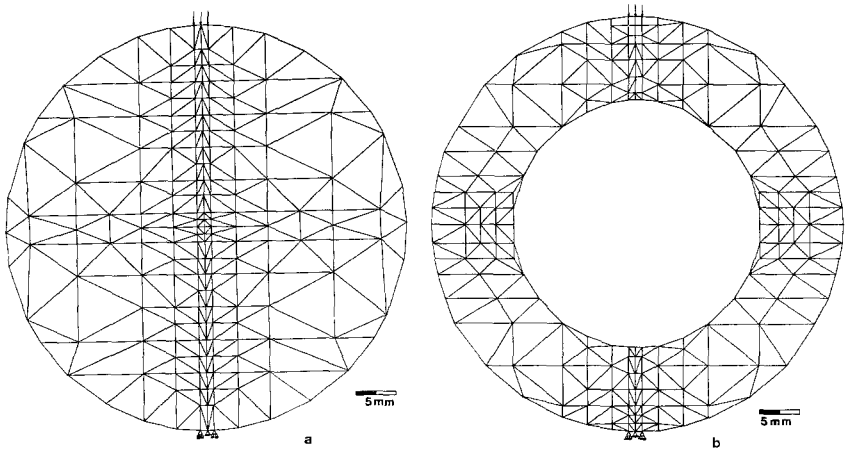

Fig. 12. Finite Element models, boundary and loading conditions: a) disc; b) ring

Finite-Element-Methode: a) Scheibenmodell mit Angabe der Belastung und Stützpunkte; b) Ringmodell

Solution avec la méthode des éléments finis: a) modèle du disque avec les conditions de charge et d'appui; b) modèle de l'anneau

loading conditions, shown in this figure, were chosen in order to represent closely the testing conditions.

a) Isotropic models

Under the assumption of homogeneity, isotropy and linear elasticity for the rock material, the stresses in a disc and in a ring were evaluated first in order to compare the finite element and the classical results. The theoretical tensile stress at the disc center is found to be 6 per cent higher than that determined by the finite element method. The value given by the finite element analysis for the coefficient to be used in the ring test is compared in Table 4 with that due to other Authors (Addinall and Hackett, 1964; Hobbs, 1964; Hiramatsu and Oka, 1970).

b) Anisotropic models

The disc model was then run by giving the material constants the values reported in Table 1 and varying the angle β at a 15 degrees interval. A representative load P of 1000 kg was applied to each model.

Table 4. Isotropic Rock: Coefficient K_r

Coefficient K_r (for $D_1/D_2 = 0.6$)	References
32.8	Addinall and Hackett, 1964
19.7	Hobbs, 1964
23.0	Hiramatsu and Oka, 1970
26.0	Present paper

The tensile stress σ_t obtained in each case at the disc center is shown in Fig. 13 as a function of β. It is observed, by a comparison with the results obtained under the assumption of isotropy, that the angle β has a definite

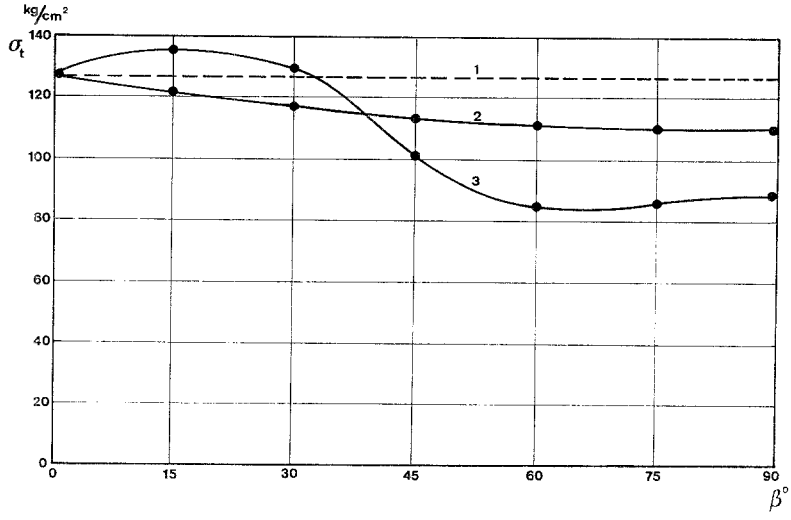

Fig. 13. Finite Element results: tensile stress σ_t at the disc center vs. the angle β
1. Isotropic case; 2. Anisotropic case, $E_1/E_2 = 1.12$; 3. Anisotropic case, $E_1/E_2 = 2.0$

Finite-Element-Methode: Beziehung zwischen der Zugspannung im Mittelpunkt der Scheibe und β
1. Isotropie; 2. Transversalisotropie, $E_1/E_2 = 1.12$; 3. $E_1/E_2 = 2.0$

Solution avec la méthode des éléments finis. Ordonnées: contraintes de traction σ_t dans le centre du disque; abscisses: β
1. Solution isotrope; 2. Solution à isotropie transversale, $E_1/E_2 = 1.12$; 3. Solution, $E_1/E_2 = 2.0$

influence on the value of this stress. Generally higher changes of σ_t correspond to higher ratios between the elastic moduli ($E_1/E_2 = 2$) (i. e. higher anisotropy of deformability). The minimum principal stress σ_2 obtained in each case

along the loading diameter is depicted in Fig. 14, where a comparison with the curve corresponding to isotropy is also shown.

Only the ring model with a higher ratio between the elastic moduli was run, by varying again the angle β at a 15 degrees interval and now setting the load P as equal to 100 kg. The tensile stress at the inner surface of the ring, where it attains its maximum value, is represented in Fig. 15 as a

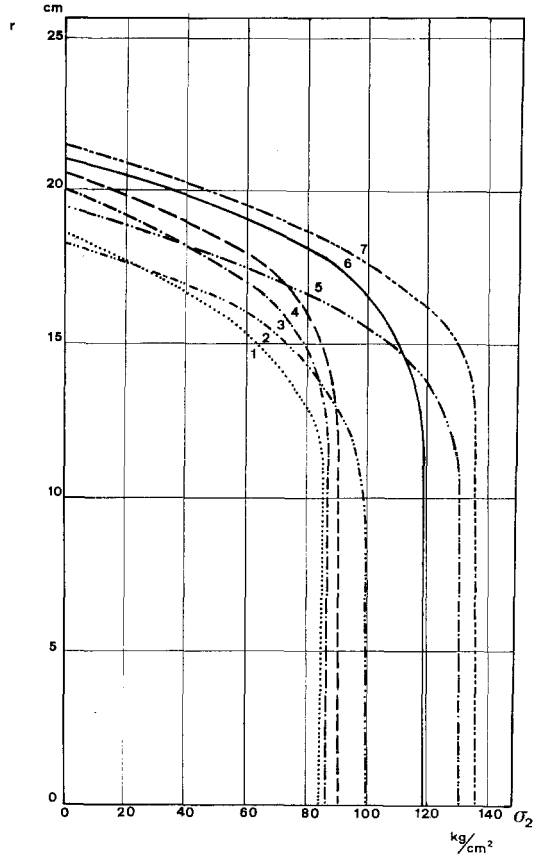

Fig. 14. Finite Element results: minimum principal stress σ_2 along the disc diametral loading direction. 1. $\beta=60^0$; 2. $\beta=45^0$; 3. $\beta=75^0$; 4. $\beta=90^0$; 5. $\beta=30^0$; 6. isotropic; 7. $\beta=15^0$

Finite-Element-Methode: Querspannungen σ_2 längs des vertikalen Durchmessers der Scheibe 1. $\beta=60^0$; 2. $\beta=45^0$; 3. $\beta=75^0$; 4. $\beta=90^0$; 5. $\beta=30^0$; 6. Isotropie; 7. $\beta=15^0$

Solution avec la méthode des éléments finis: contraintes horizontales σ_2 le long du diamètre du disque dans le plan d'action de la force P 1. $\beta=60^0$; 2. $\beta=45^0$; 3. $\beta=75^0$; 4. $\beta=90^0$; 5. $\beta=30^0$; 6. Isotropie; 7. $\beta=15^0$

function of β. The variation of the horizontal stress σ_x over the loaded diameter is depicted in Fig. 16. According to both figures, the rock anisotropy is observed to play a major role in determining different behavior patterns with respect to the isotropic case.

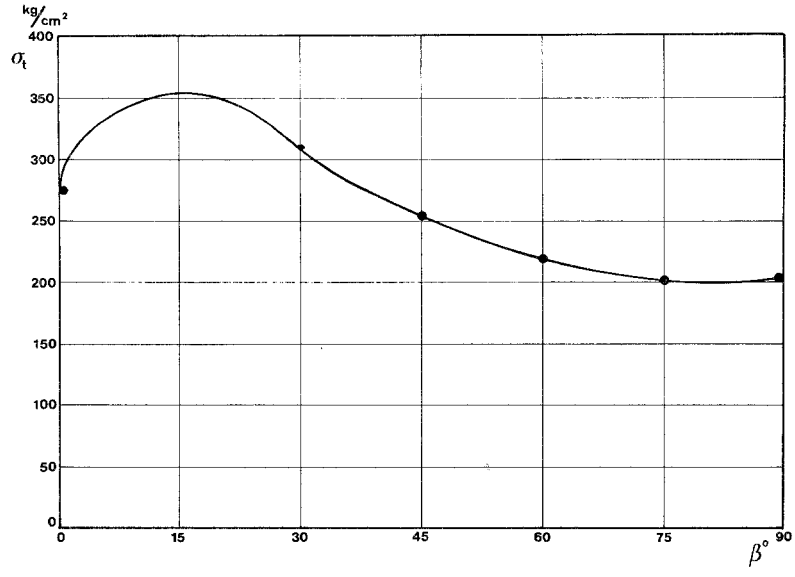

Fig. 15. Finite Element results: tensile stress σ_t at the inner surface of the ring vs. β ($E_1/E_2=2.0$)
Finite-Element-Methode: Beziehung zwischen der Zugspannung σ_t beim inneren Rand des Ringes und β
Solution avec la méthode des éléments finis: contraintes de traction σ_t sur le bord interne de l'anneau ($E_1/E_2=2.0$) en fonction de β

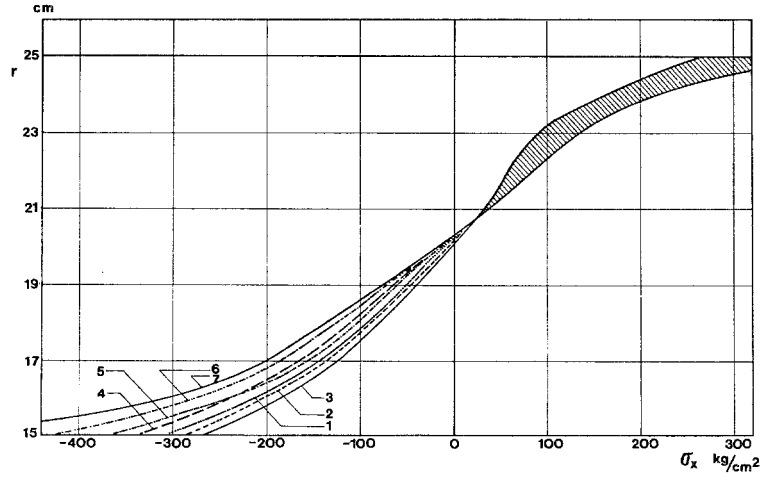

Fig. 16. Finite Element results: horizontal stress σ_x along the ring diametral loading direction
1. $\beta=60^0$; 2. $\beta=75^0$; 3. $\beta=90^0$,; 4 $\beta=45^0$; 5. isotropic; 6. $\beta=30^0$; 7. $\beta=15^0$
Finite-Element-Methode: Verteilung der Spannung σ_x in Abhängigkeit von der Dicke der Ringe in der Belastungsebene
1. $\beta=60^0$; 2. $\beta=75^0$; 3. $\beta=90^0$; 4. $\beta=45^0$; 5. Isotropie; 6. $\beta=30^0$; 7. $\beta=15^0$
Solution avec la méthode des éléments finis: contraintes dans l'épaisseur de l'anneau dans le plan d'action de la force P
1. $\beta=60^0$; 2. $\beta=75^0$; 3. $\beta=90^0$; 4. $\beta=45^0$; 5. isotropie; 6. $\beta=30^0$; 7. $\beta=15^0$

Discussion

It is of interest to compare the theoretical results of Fig. 13 (curve 2) with those given in Fig. 2, which were obtained by means of the experiments performed on the granitoidic gneiss. It is observed that the two curves show a similar trend of behavior: both the tensile stress σ_t at the disc center and the ratio P_f/Dt decrease with β.

The experimental results have given sufficient evidence supporting a tensile type of failure. Thus, the theoretical results (see Table 5, column 3)

Table 5. Finite Element Results for the Disc ($E_1/E_2 = 1.12$)

β (°)	Load at failure (P_f, kg)	Calculated tensile stress (σ_t, kg/cm²)*	Calculated tensile stress at failure (T_0, kg/cm²)	Parameter K_d
0 (isotropy)	890	127	93.0	0.634
15	760	121	74.0	0.605
30	690	117	75.0	0.590
45	655	113	59.0	0.565
60	635	110	58,5	0.550
75	640	109	55.8	0.540
90	650	107	64.0	0.590

* For the finite element computations the following is assumed: $P = 1000$ kg, $D = 50$ mm, $t = 10$ mm.

can be used to compute, for each value of β, the tensile stress at the disc center which corresponds to the load P_f at failure, i. e. the tensile strength T_0 (see Table 5, column 4).

The parameter K_d which allows one to determine the tensile strength T_0 as a function of β can also be evaluated as shown in Table 5

$$K_d = \frac{T_0 t D}{P_f}$$

A similar line of reasoning can be followed for the ring test, as an attempt can again be made to correlate the theoretical results of Fig. 15 with the experimental results for the schist, given in Fig. 8 (curve 1). One can compute the tensile stress at the inner surface of the ring which should be present at failure, i. e. the tensile strength T_0, and write (Table 6)

$$K_r = \frac{T_0 D_1 t}{P_f}$$

which is a parameter to be used for computing the tensile strength as a function of β.

On the basis of the results given above for K_d and K_r, it is concluded that the tensile strength T_0 can be evaluated as a function of β if the geometry of the specimen and the load P_f, at failure, are known for each value

Table 6. Finite Element Results for the Ring ($E_1/E_2 = 2.0$)

β (°)	Load at failure (P_f, kg)	Calculated tensile stress (σ_t, kg/cm²)*	Calculated tensile stress at failure (T_0, kg/cm²)	Parameter K_r
0 (isotropy)	100	334	265	26.0
15	94	470	365	37.0
30	82	422	255	30.5
45	70	360	199	28.0
60	59	305	143	24.0
75	54	282	124	22.5
90	60	270	129	21.2

* For the finite element computations the following is assumed: $P = 100$ kg, $D_1/D_2 = 0.6$, $t = 10$ mm.

of β. This is true, provided that the anisotropy of deformability (i. e. E_1/E_2 and ν_1/ν_2) is the same for theory and experiment.

Conclusions

The indirect tensile testing of anisotropic rocks has been investigated on experimental and theoretical basis. Both the diametral compression of circular discs and rings have been considered.

The finite element method has allowed one to determine the tensile strength of anisotropic rocks as a function of the inclination of the laminations with respect to the direction of loading.

Depending upon the type of failure which is observed in testing, either the disc or the ring test are used to provide the experimental values needed to define the tensile strength.

References

[1] Addinall, E., and P. Hackett: Tensile failure in rock-like materials. Proc. Sixth Symposium on Rock Mech., Univ. of Missouri at Rolla, Rolla, 515—538, 1964.

[2] Barron, K.: Brittle fracture initiation in and ultimate failure of rocks, Part III — Anisotropic rocks: experimental results. Int. J. Rock Mech. Min. Sci. *8*, 565—575, 1971.

[3] Fine, J., and G. Vouille: L'anisotropie des roches — Son influence sur l'essai brésilien. Revue de l'Industrie Minerale, 5—12, 1970.

[4] Hiramatsu, Y., and Y. Oka: Disc Test, Ring Test, Rectangular Plate Test and Irregular Specimen Test for Determining the Tensile Strength of Rocks. Proc. Second Congress of the International Society for Rock Mechanics, Belgrade, 199—206, 1970.

[5] Hobbs, D. W.: The Tensile Strength of Rocks. Int. J. Rock Mech. Min. Sci. *1*, 385—396, 1964.

Addresses of the authors: Prof. G. Barla, Istituto di Arte Mineraria, Politecnico, Torino, Italy; N. Innaurato, Centro di studio per i problemi minerari del C. N. R., Politecnico, Torino, Italy.